Chapter 26

Kryptoracemates

Edward R.T. Tiekink

Research Centre for Crystalline Materials, School of Science and Technology, 5 Jalan Universiti, Sunway University, Bandar Sunway, Selangor Darul Ehsan 47500, Malaysia

e-mail edwardt@sunway.edu.my

Abstract

Racemic crystals normally crystallise in centrosymmetric space-groups containing equal numbers of enantiomers. More rarely, racemates may crystallise in non-centrosymmetric space-groups having glide symmetry or, even more rarely, in space-groups devoid of a centre of inversion, having no rotary-inversion axes nor glide plane. The latter class of crystals form the subject of the present bibliographic review – a survey of kryptoracemic behaviour. The term kryptoracemic alludes to the presence of a hidden or non-crystallographic centre of inversion between two molecules that might otherwise be expected

to crystallise in an achiral space-group, often about a centre of inversion. Herein, examples of molecules with stereogenic centres crystallising in one of the 65 Sohncke space-groups are described. Genuine kryptoracemates, *i.e*. crystals comprising only enantiomorphous pairs are described followed by an overview of non-genuine kryptoracemates whereby the crystal also contains other species such as solvent and/or counterions. A full range, *i.e*. one to six, stereogenic centres are noted in genuine kryptoracemates. Examples will also be described whereby there are more that one enantiomeric pair of molecules in the crystallographic asymmetric unit. A more diverse range of examples are available for non-genuine kryptoracemates. There are unbalanced species where in addition to the enantiomeric pair of molecules, there is another enantiomeric molecule present. There are examples of genuine co-crystals, solvated species and of salts. Finally, special examples will be highlighted where the counterions are chiral and where they are disparate, both circumstances promoting kryptoracemic behaviour.

Keywords Kryptoracemate • Molecular packing • Crystal structure • Crystallisation • Chirality

26.1 Introduction

The intriguing term *kryptoracemate* has been ascribed [1] to Ivan Bernal, a renowned chemical crystallographer with a particular interest in chirality in crystals especially in metalorganic systems. It is understood that Ivan Bernal employed the term during a meeting of the American Crystallographic Association in the mid-1990's [2]. Clearly, the term refers to the crystallisation of racemic compounds. Less obvious is the origin of the prefix "*krypto*", which comes from the Greek and loosely translates as hidden. Thus, kryptoracemic behaviour refers to crystallisation of racemic molecules about a hidden, *i.e.* a non-crystallographic, centre of inversion. For organic molecules, the most recent comprehensive review of the topic by Fábián and Brock [3] highlights how rare this phenomenon is, accounting for only 0.1% of all-organic structures included in the Cambridge Structural Database (CSD) [4]; a complimentary survey of kryptoracemic behaviour in metalorganic systems has been published by Bernal and

Watkins [5]. The aim of the present Chapter is to alert the reader to this crystallographic peculiarity by surveying the structural characteristics of representative examples of all-organic molecules known with a certain degree of confidence to exhibit kryptoracemic behaviour.

There are at least three possible outcomes from the crystallisation from a solution of a racemic compound. In descending order of importance, these crystallisation outcomes are: i) an ordered racemic crystal, ii) a physical mixture comprising equal numbers of enantiopure crystals and iii) a kryptoracemate; herein, solid-solutions and enantiomorphous twins are ignored. Racemic compounds have equal numbers of the enantiomers in the crystal, *i.e*. an equal distribution of mirror images of the molecules. This is normally accomplished by having the molecules disposed about a crystallographic centre of inversion. There are exceptions to this general principle whereby a racemate can crystallise in a non-centrosymmetric space-group, but a space-group having glide symmetry so that the criterion of having equal numbers of mirror images pertains. An early survey of this later phenomenon by Dalhus and Görbitz [6] revealed that 90% of crystals in this category crystallised in five non-centrosymmetric space-

groups, namely *Pc*, *Cc*, *Pca*2$_1$, *Pna*2$_1$ and *Fdd*2. The second phenomenon leading to a physical mixture of crystals, or a conglomerate of homo-chiral crystals, is usually termed spontaneous resolution and was famously recognised by Pasteur in his work on ammonium sodium tartrate crystals [7]. The third crystallisation outcome for racemic compounds results in kryptoracemic crystals which are characterised as crystallising in space-groups lacking a centre of inversion, mirror planes and rotary-inversion centres, *i.e.* not having symmetry operators of the second kind, as discussed further below.

The reality is that most organic materials containing a pair of resolvable isomers (also those with meso symmetry and achiral compounds) crystallise in one of the centrosymmetric space-groups leading to hetero-chiral crystals; this has been termed an enantiophilic trait [8]. It is estimated that 99% of molecules (neutral and charged) that can crystallise in a centrosymmetric space-group, will do so [9]. This is probably related to close-packing considerations: it is well established that 83% of all structures included in the CSD [4] crystallise in one of six space-groups out of a possible 230 space-groups (or 219 when the 11 pairs of enantiomorphic space-groups are counted once

only), *i.e.* $P2_1/c$ (34.6%), $P\bar{1}$ (24.5%), $C2/c$ (8.4%), $P2_12_12_1$ (7.2%), $P2_1$ (5.2%) and *Pbca* (3.3%), or alternative settings of these [9, 10]. The common feature of the indicated space-groups is that they are all are conducive to close-packing arrangements, which is optimised for spherical molecules. Thus, an odd-shaped molecule crystallising about a centre of inversion inherently becomes more spherical in shape. When, enantiophilic behaviour [8] no longer prevails, enantiophobic behaviour comes to the fore resulting in the formation of conglomerates or, more rarely, kryptoracemates.

In terms of space-group symmetry, kryptoracemates are restricted in the adoption of these. As mentioned above, kryptoracemates can only crystallise in space-groups not having symmetry operators of the second kind. Thus, a kryptoracemate must crystallise in one of the 65 Sohncke space-groups (non-enantiogenic groups) which are characterised as not having a centre of inversion, rotary-inversion axes or glide planes, *i.e.* only have symmetry operations of the first kind; crystals adopting Sohncke space-groups are chiral. Further, the number of molecules in the crystallographic asymmetric unit, *i.e.* Z' (equals the number of formula units in a unit cell divided by the

number of general positions for that unit cell) is greater than unity unless the molecule itself lies on a rotation axis [11].

The purpose of this overview is not to give a comprehensive list of all known kryptoracemates but, rather highlight the different classes of kryptoracemates that have been described in the crystallographic literature. As a starting point, a clarification of the term kryptoracemic compound is made, analogous to that now adopted for supramolecular isomers [12, 13]. A supramolecular isomer (SI) is a molecule/framework that can adopt a different structure, including with different atomic connectivity, as opposed to a polymorph [14]. Often, this phenomenon was accompanied by a change in the counter-ion and/or solvent occluded in the crystal [12]. Subsequently, the term was modified to refer to a genuine SI [13], whereby the molecular formula was exactly the same, rather than the generic, all-encompassing SI [12]. Thus, herein, kryptoracemates are divided into "genuine kryptoracemates", with only one type of species (molecule or zwitterion) in the crystal, and "more loosely-defined kryptoracemates", which may include counter-ions, solvent, *etc*. in their crystals.

With the above division in mind, the following survey is arranged in terms of the number of chiral centres in the molecule and highlights different issues associated with the examples, for example, polymorphism, the availability of crystals of diastereoisomers, *etc*. The images herein are original, being generated from the Crystallographic Information Files (CIF's) [15] available through the CSD [4] employing DIAMOND [16] and Qmol [17]. The chemical diagrams were drawn with ChemDraw™ and data analysis was aided by Mercury [18] and PLATON [19]. The respective CSD [4] REFCODES are included in the captions to the figures. Finally, while common names are employed in the text as much as possible, IUPAC names are included in the captions to the figures, as determined by MarvinSketch [20].

26.2 Genuine kryptoracemates

A distinction is made herein between genuine and non-genuine kryptoracemates. While the basic definition is the same for both classes of compound, the influence of solvent or a counterion on the crystallisation outcome is virtually impossible to determine with absolute

confidence. Hence, kryptoracemic crystals comprising enantiomorphic molecules are discussed first; in 26.3, kryptoracemic crystals having additional species present in the crystal will be described.

One of the very first molecules to exhibit kryptoracemic behaviour was DL-2-hydroxyphenylalanine (**1**), which, in fact crystallises as a zwitterion [21]; images for **1** are shown in Figure 26.1. There is one stereogenic centre in **1**, which crystallises in the monoclinic space-group $P2_1$ with $Z' = 2$, the asymmetric unit comprising a pair of ostensibly enantiomorphic molecules; the *S* form is shown in Figure 26.1. The overlap diagram, comprising the *S*-form and inverted *R*-form display an almost perfect overlap, as is often seen in kryptoracemates. However, in this case, the diagram is misleading. The enantiomeric molecules are related by a non-crystallographic centre of inversion located at 0.661, 0.390, 0.802. As the fractional atomic coordinates for the *R*-form were not available, this molecule was generated arbitrarily. While **1** is zwitterionic, the overwhelming majority of genuine kryptoracemates comprise neutral enantiomers.

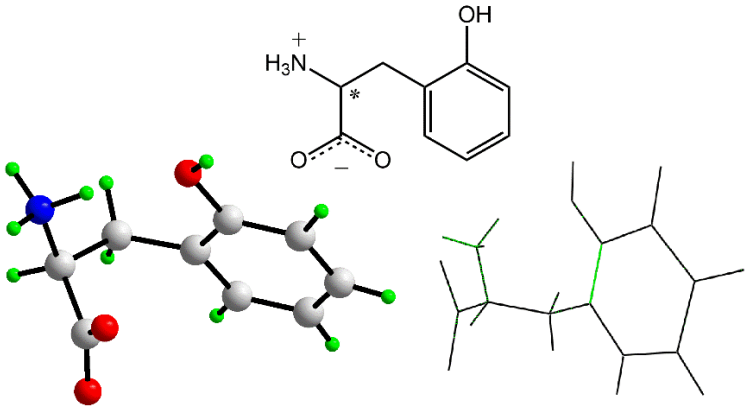

Figure 26.1. Images for 2-azaniumyl-3-(2-hydroxyphenyl)propanoate (DTYROS), **1**: chemical diagram (upper view), molecular structure \ and overlay diagram.

Figure 26.2 shows images for 4-azido-5-(biphenyl-4-yl)-5-hydroxy-3-methyl-2-oxo-2,5-dihydrofuran (**2**), a neutral molecule crystallising with $Z' = 2$ (space-group $P2_1$); the *R*-form is illustrated in the molecular diagram [22]. The overlap diagram highlights a close correspondence of the molecular structures in the independent tetrahydrofuranyl rings (*R*- and inverted-*S* forms) but differences in the orientations of the biphenyl residues.

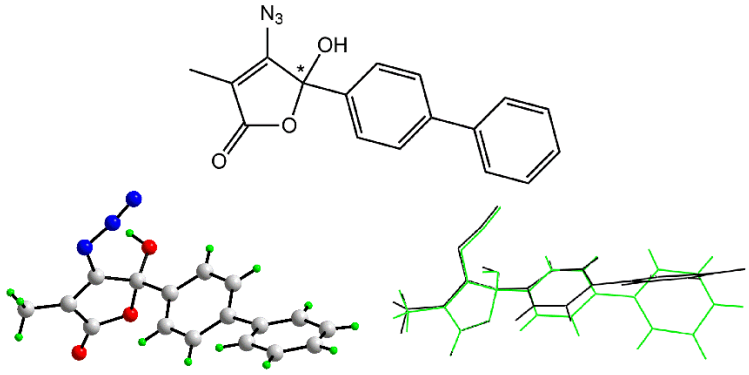

Figure 26.2. Images for 4-azido-5-hydroxy-3-methyl-5-(4-phenylphenyl)-2,5-dihydrofuran-2-one (DIXPUW), **2**: chemical diagram, molecular structure and overlay diagram.

In **3**, 2,4-dinitro-2,3-dichloro-3-thiolene-1,1-dioxide, rich in heteroatoms, a close overlap is again noted between the five-membered rings when the molecule in Figure 26.3, *i.e.* the *S*-form, is overlapped with the inverted form [23]. The molecule crystallises in the orthorhombic space-group $P2_12_12_1$ with $Z' = 2$.

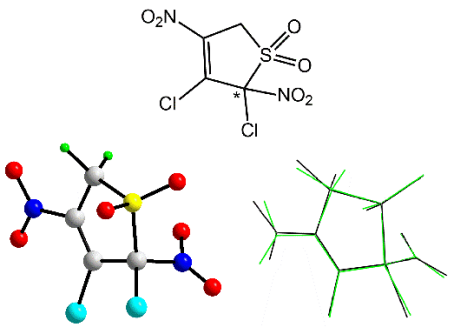

Figure 26.3. Images for 2,3-dichloro-2,4-dinitro-2,5-dihydro-1λ^6-thiophene-1,1-dione (LACFEB), **3**: chemical diagram, molecular structure and overlay diagram.

Kryptoracemic behaviour is not restricted to examples with Z' = 2, *i.e*. two independent molecules in the crystallographic asymmetric unit. This is illustrated for 1,6-dihydro-1,6-dimethyl-4-phenyl-1,2,3-triazine 2-oxide (**4**), where Z' = 4 (monoclinic, $P2_1$); **4** is another example of a formally charged species [24]. The asymmetric unit of **4** comprises two independent pairs of enantiomeric molecules, neither of which is related by crystallographic symmetry. The illustrated molecule in Figure 26.4 has the chiral centre being *R*. Thus, there are one further *R*-form and two *S*-forms in the asymmetric unit. The overlap diagram of the two *R*-forms with the inverted *S*-forms reveal high degree of concordance among the four independent molecular conformations.

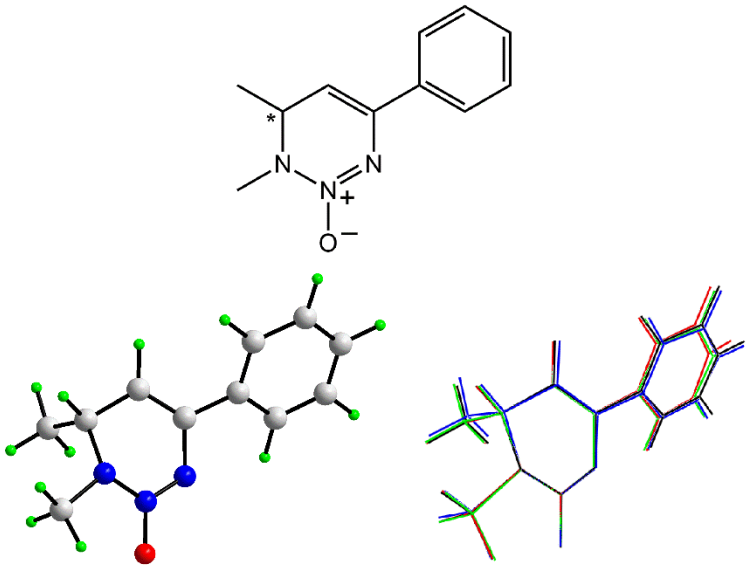

Figure 26.4. Images for 1,6-dimethyl-4-phenyl-1,6-dihydro-1,2,3-triazin-2-ium-2-olate (FATFUB), **4**: chemical diagram, molecular structure of and overlay diagram.

Molecules of 8-methoxy-1-oxacyclotetradeca-2,13-dione (**5**) have a single stereogenic centre, with the *S*-form shown in Figure 26.5. The kryptoracemate crystallises in the monoclinic space-group $P2_1$, $Z' = 2$ [25]. A centrosymmetric polymorph is also known for **5**, which exhibits similar unit cell parameters for the space-group $P2_1/c$, $Z' = 1$ [26]. The overlay diagram highlights the close agreement in the molecular conformations. The above observations raise two

crucial issues when assessing the aetiology and even the validity of kryptoracemic behaviour.

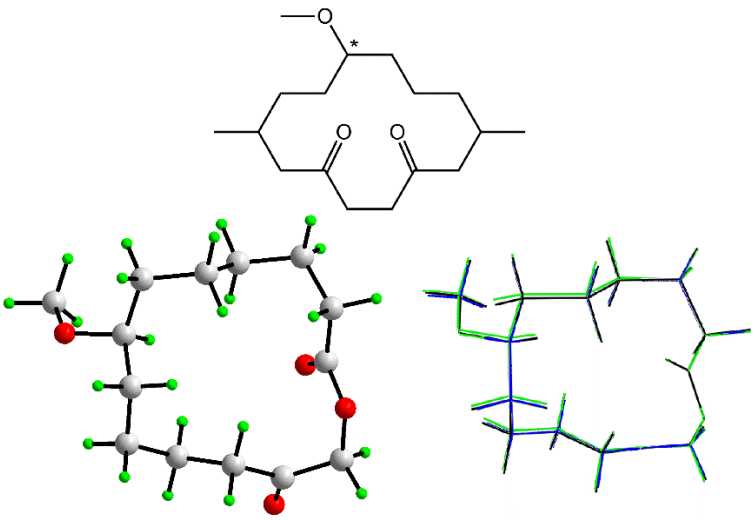

Figure 26.5. Images for 8-methoxy-1-oxacyclotetradecane-2,13-dione (NIWHUX), **5**: chemical diagram, molecular structure and overlay diagram. In the latter, the blue trace represents the molecule found in the centrosymmetric crystal [26].

The first important issue to be addressed relates to the correctness of the assigned space-group. In a series of publications spanning several decades [28], Marsh and colleagues periodically corrected space-group assignments. Particularly relevant to the present survey was the conclusion that the most often missed symmetry in space-

group assignments, often leading to incorrect or even over-interpretation of chemistry/correlations with spectroscopy, was the presence of a centre of inversion [29]. With modern software, such as PLATON [19], it is likely that the number of errant structures will be/should be reduced.

The question of mis-assigned space-groups notwithstanding, the second issue arising from the appearance of non-centrosymmetric and centrosymmetric polymorphs for **5**, remains largely unanswered. The crux of this question is: why do kryptoracemates appear in the first place? The centrosymmetric structure of **5** indicates that enantiomers of **5** can and do crystallise in a centrosymmetric space-group, as might be expected. So, why the appearance of a non-centrosymmetric version, the kryptoracemate? As noted above, kryptoracemates crystallise with $Z' > 1$; thus far, the author has not come across a kryptoracemate with the molecule lying on a rotation axis. Thus, kryptoracemates may be considered a special case of the relatively large number of structures with $Z' > 1$. In a recent comprehensive review of this topic, Steed and Steed [30] indicate that 9% of all-organic crystals have $Z' > 1$ and include reasons for this phenomenon

such as having awkward-shaped molecules, the vagaries of crystallisation techniques, thermodynamics, *etc*. or some combination of these. In the case of **5**, it might be that the observation of the kryptoracemic form may be the result of a rapid crystallisation, the kinetic form, and the centrosymmetric form, the thermodynamic outcome.

Thus far, all of the discussed kryptoracemates discussed feature a single steroegenic centre only. However, two and more stereogenic centres may be found in kryptoracemates. An example of a kryptoracemate with two stereogenic centres is illustrated for 2,2'-dimethyl-2,2',3,3'-tetrahydro-1,1'-bicyclopenta(a)naphthalenylidene (**6**) [31] in Figure 26.6. In the illustrated molecule, both chiral centres are *R*. As seen above, the superimposition of the illustrated molecule with the inverted form shows a close correlation with the exception of the relative orientations of the methyl substituents.

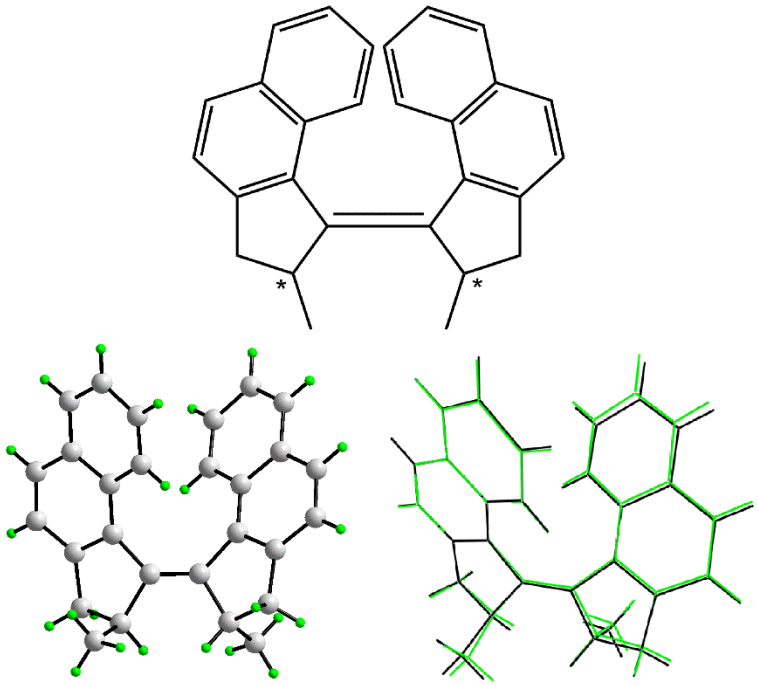

Figure 26.6. Images for 2-methyl-1-{2-methyl-1H,2H,3H-cyclopenta[a]naphthalen-1-ylidene}-1H,2H,3H-cyclopenta[a]naphthalene (AQABID, **6**): chemical diagram, molecular structure and overlay diagram.

In 2-[(3,5-dinitrobenzene)amido]cyclobutane-1-carboxylic acid (**7**) [32], the configurations at the sp^3-carbon atoms bearing the carboxylic acid and amino functionalities are *R* and *S*, respectively, as shown in Figure 26.7. The overlap diagram again confirms the close

similarity in the molecular conformations, especially in the four-membered rings. The presence of carboxylic acid functionality might be expected to promote the formation of a racemic crystal whereby the carboxylic acid groups of each enantiomer associates about a centre of inversion *via* the familiar eight-membered $\{\cdots HOCO\}_2$ homo-synthon. However, while the $\{\cdots HOCO\}_2$ homo-synthon is formed between the two molecules in the crystal (orthorhombic, $P2_12_12_1$), the homo-synthon is non-symmetric. It is worth noting here that it is well established in the crystallographic literature that carboxylic acids form the eight-membered $\{\cdots HOCO\}_2$ homo-synthon in only about a third of the crystal structures where this is possible, being heavily susceptible to competing supramolecular synthons [33, 34].

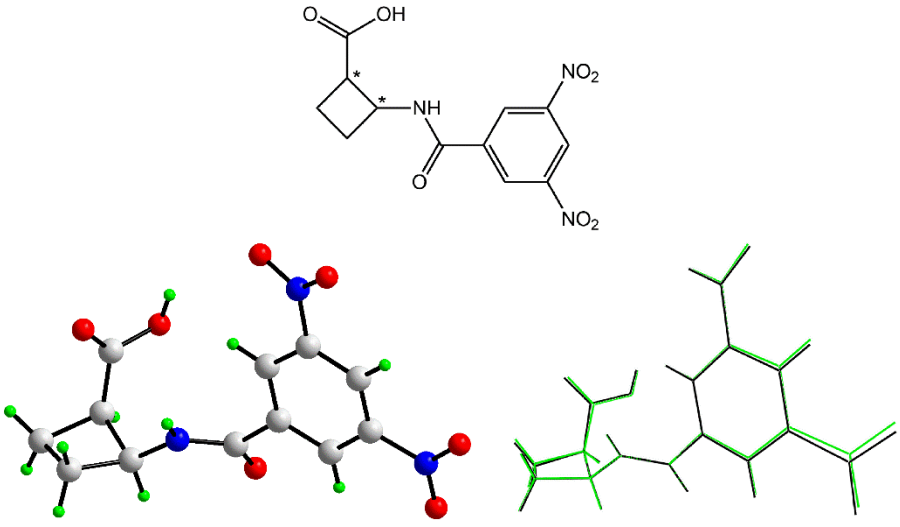

Figure 26.7. Images for 2-[(3,5-dinitrobenzene)amido]cyclobutane-1-carboxylic acid (EGURIH; **7**): chemical diagram, molecular structure and overlay diagram.

In another variation of the theme, thus far, all of the chiral centres have been carbon based. An attractive exception is found in the triphosphatricyclohexadecatriene derivative (**8**) [35]; the crystal is monoclinic, $P2_1$. As seen from Figure 26.8, the two chiral centres are phosphorus-based with the configuration being *S* at the phosphorus centre bearing the chloride substituents and *R* at the second chiral phosphorus atom. Unlike several other structures, differences between the enantiomers are noted in the conformations of the nine-membered rings and in the relative orientations of two phenyl rings.

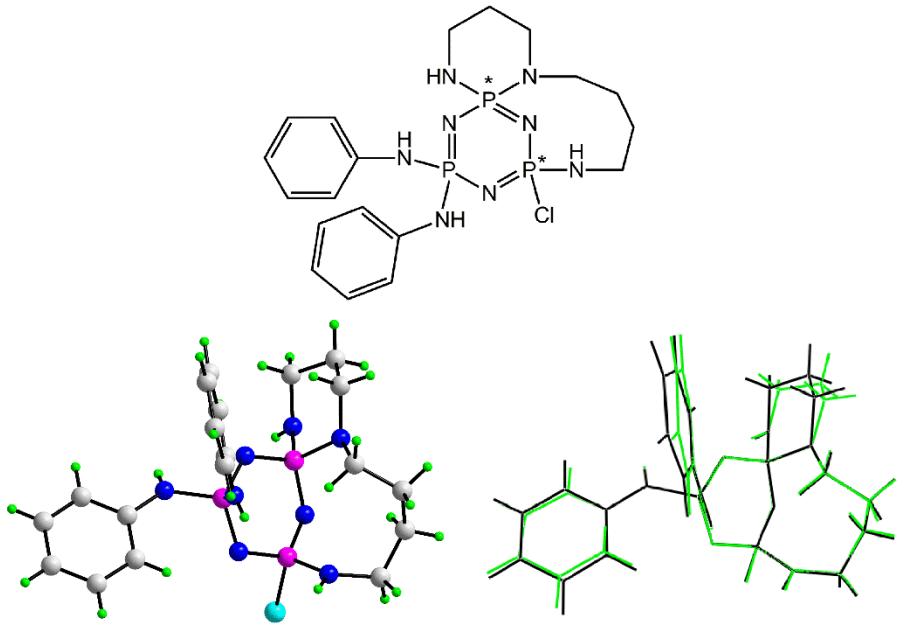

Figure 26.8. Images for 12-chloro-14-N',14-N-diphenyl-2,6,11,13,15,16-hexaaza-1λ^5,12λ^5,14λ^5-triphosphatricyclo[10.3.1.0^{1,6}]hexadeca-1(16),12,14-triene-14,14-diamine (GAFJIH; **8**): chemical diagram, molecular structure and overlay diagram.

Three chiral centres are noted in the crystal of 1-acetoxy-7-cyano-5-methylbicyclo(3.2.0)heptan-2-one (**9**) [36]. For the illustrated molecule in Figure 26.9, which crystallises in the monoclinic

space-group $P2_1$, the configurations at the acetyl, cyano and methyl-substituted carbon atoms are *R*, *R*, and *S*, respectively.

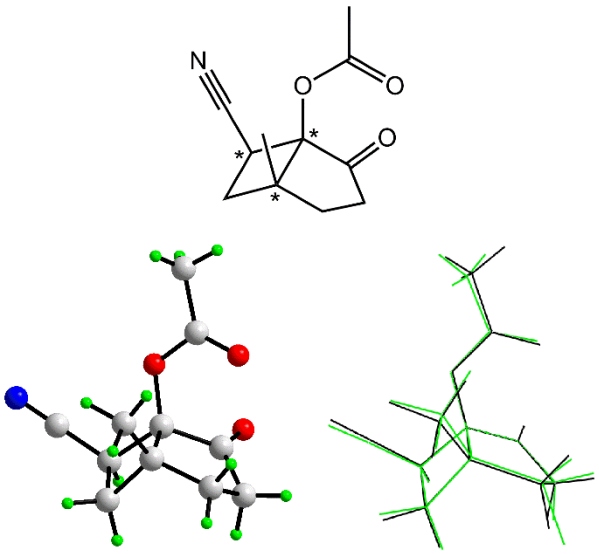

Figure 26.9. Images for 7-cyano-5-methyl-2-oxobicyclo[3.2.0]heptan-1-yl acetate (BINGOU; **9**): chemical diagram, molecular structure and overlay diagram.

The structure of 6a-ethyl-1-(phenylsulfonyl)decahydro-4H-pyrrolo(3,2,1-ij)quinoline (**10**) [36] is notable for two reasons. First and foremost, there are four chiral centres in the molecule, see Figure 26.10. The configurations about the centres bearing sulphur and

nitrogen atoms are each *S* while those about the carbon atoms bound to three carbon atoms are each *R*. Secondly, the crystal structure of a stereoisomer is known. The stereoisomer crystallises in the centrosymmetric space-group $P2_1/c$ with $Z' = 1$ with equal numbers of all *S*,*S*,*S*,*R* (and *R*,*R*,*R*,*S*) configurations [37].

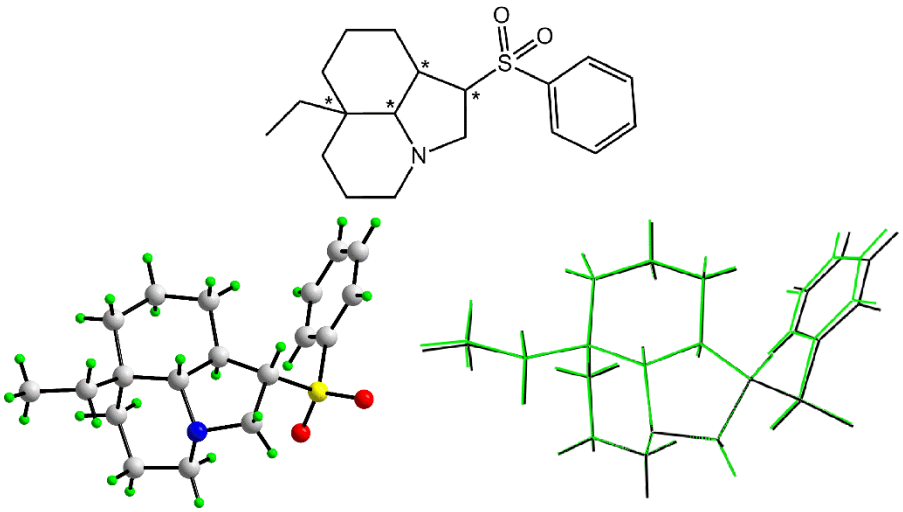

Figure 26.10. Images for 3-(benzenesulfonyl)-8-ethyl-1-azatricyclo[6.3.1.$0^{4,12}$]dodecane (HILXUW; **10**): chemical diagram, molecular structure and overlay diagram.

Kryptoracemic crystals of the di-hydroxyl species, 1,2,3,4,5,6-hexahydro-2a,4a-(ethano)cyclopenta(fg)acenaphthylene-3,9-diol (**11**) feature four chiral centres in a monoclinic crystal with space-

group $P2_1$ with $Z' = 4$ [38], *i.e.* with two pairs of crystallographic independent enantiomeric molecules. In the molecule illustrated in Figure 26.11, the two hydroxyl-bearing carbon atoms each has an *S*-configuration while the other two chiral centres each has a *R*-configuration. Further interest in **11** rests with the observation that a polymorph is also known [38]. In this monoclinic crystal, there are one and one-half independent molecules in the asymmetric unit ($Z' = 1.5$) with the space-group being $P2/c$. While one molecule lies in a general position (yellow image in the overlay diagram) while the other is located about a two-fold axis of symmetry (pink image). The overlay diagram of the six independent molecules in Figure 11 highlights only small conformational differences in the molecules.

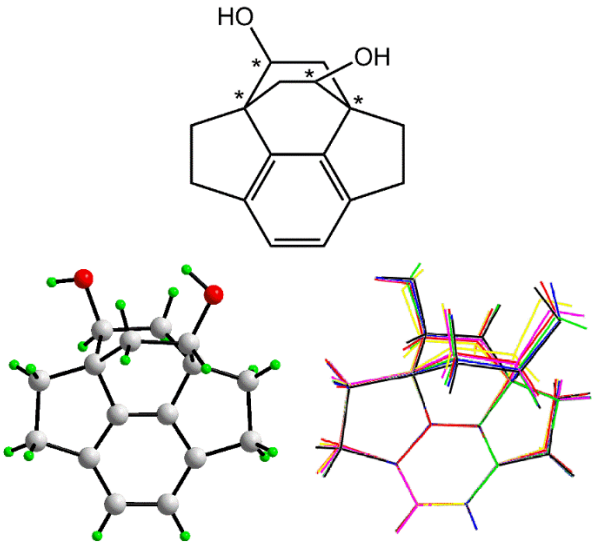

Figure 26.11. Images for pentacyclo[5.5.2.2^{1,4}.0^{4,14}.0^{10,13}]hexadeca-7(14),8,10(13)-triene-2,15-diol (NOLFUP; **11**): chemical diagram, molecular structure and overlay diagram.

The are five stereogenic centres in the dibromo derivative, 1,10-dibromotricyclo(5.2.2.02,6)undeca-4,8-diene (**12**) [39]; crystals belong to the orthorhombic space-group $P2_12_12_1$. In the illustrated molecule of Figure 26.12, the chiral centres connecting the five- and six-membered rings each have an *S*-configuration and the remaining chiral centres are each *R*.

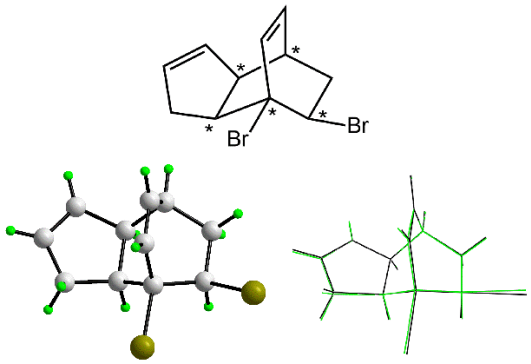

Figure 26.12. Images for 7,11-dibromotricyclo[5.2.2.$0^{2,6}$]undeca-3,8- diene (QEWTES; **12**): chemical diagram, molecular structure and overlay diagram.

The final structure to be described among the genuine kryptoracemates is that of 4,7;13,16-diepoxy-9,18-dimethyl-1,10-dioxacyclo-octadecane-2,11-dione (**13**) [40]. The molecule crystallises in the monoclinic space-group $P2_1$ and with $Z' = 4$; *i.e.* there are two pairs of enantiomeric pairs related across a non-crystallographic centre of symmetry. The illustrated molecule of **13** in Figure 26.13 has six stereogenic centres, each having a *R*-configuration. The overlap diagram of the two all *R*-species with the inverted all *S*-species show a high degree of concordance in molecular conformation.

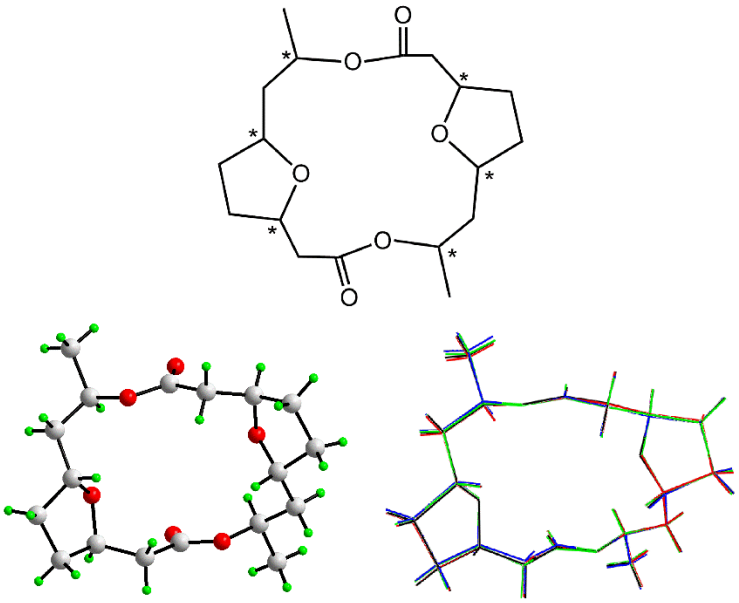

Figure 26.13. Images for 5,14-dimethyl-4,13,19,20- tetraoxatricyclo[14.2.1.1^{7,10}]icosane-3,12- dione (NUYTAC; **13**): chemical diagram, molecular structure and overlay diagram.

26.3 Non-genuine kryptoracemates

In this section, representative examples of kryptoracemates with additional species incorporated in the crystal are described. These are solvates, salts and crystals with a combination of these. Enantiomeric pairs of chiral molecules are present in all examples as for the genuine kryptoracemates reviewed in 26.2 but, so are other species. In most cases it is likely that the presence of additional species does not have

a significant influence on the observed kryptoracemic behaviour but, as will be demonstrated, certain counter-ions can be employed to force the formation of kryptoracemates.

The first structure to be described in this section may be considered the result of an unbalanced crystallisation. In the crystal of *trans*-2-N,N'-dimethylaminomethyl-1,3-dithiolane-1,3-dioxide (**14**) [41], the chiral centres are the sulphoxide-sulphur atoms, having *R*- and *S*-configurations in the molecule illustrated in Figure 26.14. The molecule crystallises in the monoclinic space-group $P2_1$ with $Z' = 3$. Two of the molecules have the conformation shown in the molecular structure diagram of Figure 26.14, and the third molecule has the opposite, *i.e*. *S*- and *R*-configurations. Hence, there is a deviation from the usual 1:1 enantiomeric ratio, and hence, the use of the term "unbalanced. In one sense, **14** can be considered a multi-component crystal of an enantiomeric pair of **14** co-crystallised with a *RS*-diastereoisomer.

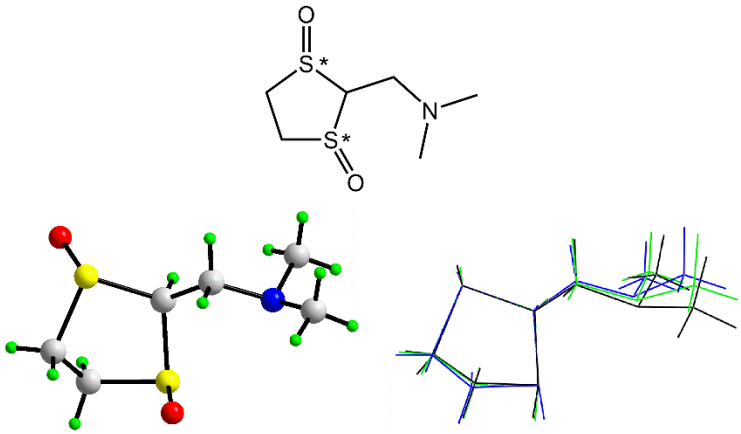

Figure 26.14. Images for 2-[(dimethylamino)methyl]-1λ^4,3λ^4-dithiolane-1,3-dione (VEFMEZ; **14**): chemical diagram, molecular structure and overlay diagram.

An analogous situation to **14** pertains in the crystal of 6-(dimethoxymethylene)-dibenzo(d,k)tricyclo(5.2.2.0^{3,7})undeca-4,10-dien-8-one (**15**) [42], which crystallises in the triclinic space-group *P*1 with *Z*′ = 4. In this unbalanced crystal, three of molecules have the configuration shown in the molecular structure of Figure 26.15, *i.e*. with *R*-configurations at the three chiral centres, and the fourth molecule has the all-*S*-configuration. Minor conformational differences in the orientations of some of the aromatic rings are noted in the

overlay diagram (the inverted all-*S*-configuration is represented by the red image).

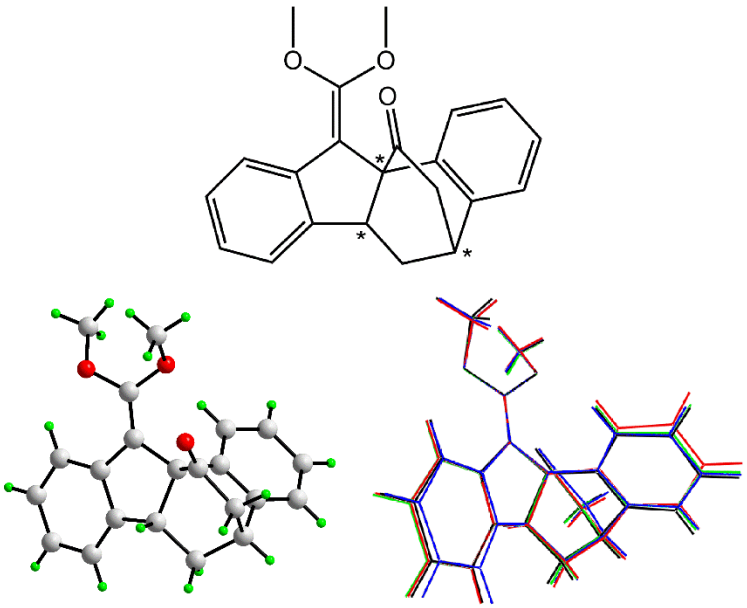

Figure 26.15. Images for 2-(dimethoxymethylidene)pentacyclo[9.6.2.$0^{1,9}$.$0^{3,8}$.$0^{12,17}$]nonadeca- 3(8),4,6,12,14,16-hexaen-18-one (SOQQOE, **15**): chemical diagram, molecular structure and overlay diagram.

A more conventional co-crystal is evident for **16**, having a 2:1 composition of 3,3-dimethyl-4-(phenylsulfonyl)azetidin-2-one and

trans-3-methyl-4-(phenylsulfonyl)azetidin-2-one; **16** crystallises in the monoclinic space-group $P2_1$ [43]. The illustrated molecule in Figure 26.16 has an *R*-configuration around the chiral centre, and the overlay diagram between it and its inverted enantiomer suggests a conformational difference associated with the relative orientations of the phenylsulphoxide residues. In the molecular packing, each of the amine-N–H atoms forms a similar weak hydrogen-bond with a sulphoxide-oxygen atom.

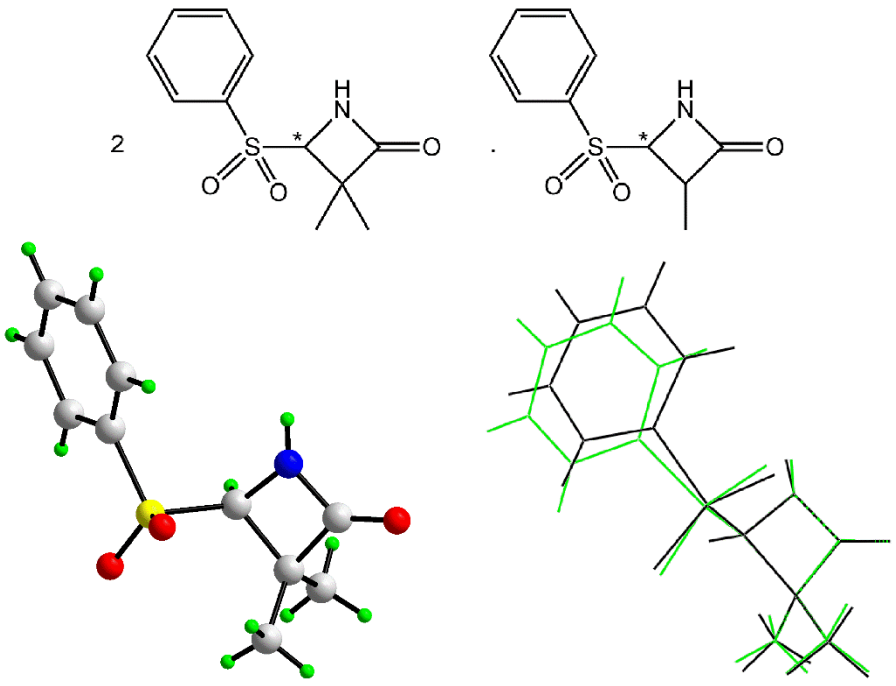

Figure 26.16. Images for the 2:1 4-(benzenesulfonyl)-3-methylazetidin-2-one 4-(benzenesulfonyl)-3,3-dimethylazetidin-2-one co-crystal (ABADUD; **16**): chemical diagram, molecular structure of 4-(benzenesulfonyl)-3,3-dimethylazetidin-2-one and overlay diagram for an enantiomeric pair of 4-(benzenesulfonyl)-3,3-dimethylazetidin-2-one molecules.

The carboxylic acid, syn-1-benzyl-4,5-diphenyl-2-methyl-4,5-dihydroimidazole-4-carboxylic acid, has been crystallised as its hemi-dichloromethane solvate (**17**) in the orthorhombic space-group $P2_12_12_1$ [44]. In the molecule illustrated in Figure 26.17, the configuration on the carbon atom bearing the carboxylic acid is *S* and the other chiral centre is *R*. The overlay diagram is exceptional in that there are significant conformational differences in all but the methyl substituents about the central five-membered imidazole ring. In the crystal, each of the hydroxyl groups forms an intermolecular hydrogen-bonding interaction with an imidazole-nitrogen atom rather than self-associating *via* hydroxyl-O–H···O(hydroxyl) hydrogen-bonding,

as has been noted previously in cases of steric congestion [45] and in the presence of competing synthons [46].

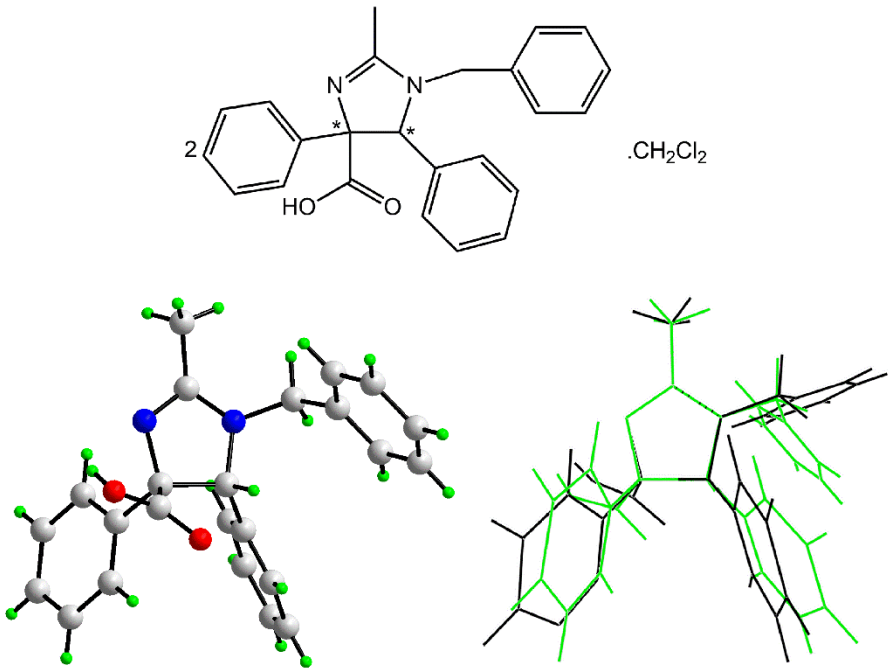

Figure 26.17. Images for 1-benzyl-2-methyl-4,5-diphenyl-4,5-dihydro-1H-imidazole-4-carboxylic acid dichloromethane solvate (2:1) (KODQOK; **17**): chemical diagram, molecular structure of the carboxylic acid and overlay diagram for the enantiomeric the carboxylic acids.

Another solvate, this time a 3:2 hydrate is found in the orthorhombic ($P2_12_12_1$) crystals of 2,8-diisopropyl-5-trifluoromethyl-7,8-

dihydro-1,12-iminobenzo(c)pyrido(4,3,2-ef)(1)-benzazepine (**18**) [47]. Just as for **15** and **16** described above, the composition of **18** can be considered as being unbalanced, with the crystallographic asymmetric unit comprising the illustrated molecule in Figure 26.18, with an *S*-configuration at the chiral centre, two inverted organic molecules along with two water molecules of crystallisation. Different orientations of the isopropyl groups are evident in the overlay diagram. The independent molecules form different intermolecular interactions. The molecule with the *S*-configuration, forms amine-N–H···N(amine) and N–H···N(pyridyl) hydrogen-bonds. By contrast, each of the two molecules with a *R*-configuration forms amine-N–H···O(water) and N–H···N(amine) hydrogen-bonds.

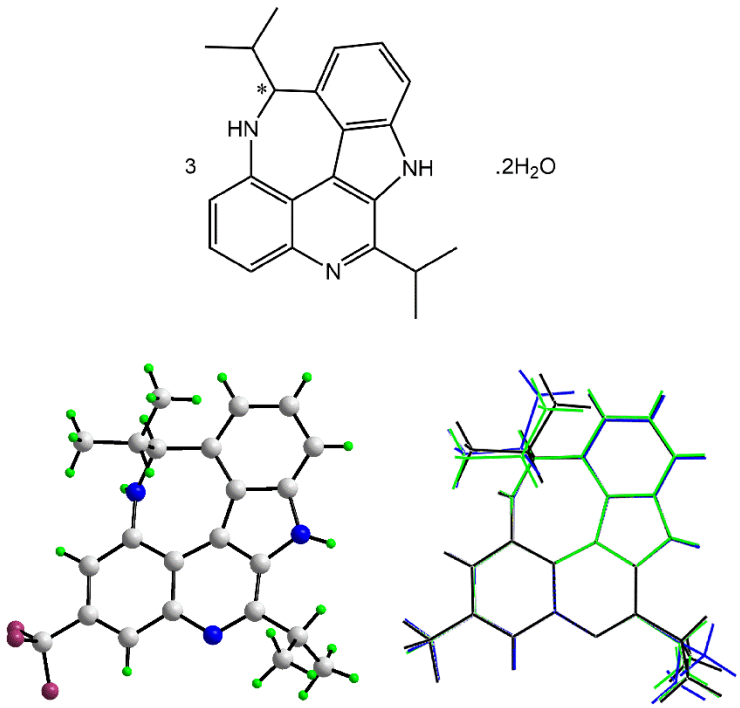

Figure 26.18. Images for the 3:2 8,16-bis(propan-2-yl)-12-(trifluoromethyl)-9,15,19-triazapentacyclo[8.7.1.1^{3,17}.0^{2,7}.0^{14,18}]nonadeca-1(18),2(7),3,5,10,12,14,16-octaene hydrate (AWUVUJ; **18**): chemical diagram , molecular structure of 2,8-diisopropyl-5-trifluoromethyl-7,8-dihydro-1,12-iminobenzo(c)pyrido(4,3,2-ef)(1)benzazepine and overlay diagram of the organic molecules.

Attention is now directed towards the description of four salts. The first of these, namely the 1:1 salt 2-amino-N-(1-methyl-1,2-

diphenylethyl)acetamide hydrochloride (**19**) [48] crystallises in the monoclinic space-group $P2_1$ with an enantiomeric pair of cations and two chloride counter-ions in the asymmetric unit. The chiral centre in the cation shown in Figure 26.19 has a *R*-configuration. As noted above for **17**, non-trivial conformational differences are evident for the pendant groups in the overlay diagram. There is charge-assisted ammonium-N–H···Cl and ammonium-N–H···O(carbonyl) along with amino-N–H···Cl and amino-N–H···O(carbonyl) hydrogen-bonding operating in the molecular packing. The independent cations have distinctive hydrogen-bonding patterns, with the molecule shown in Figure 26.19 forming ammonium-N–H···Cl and amino-N–H···O(carbonyl) hydrogen-bonds as opposed to the enantiomer which forms two ammonium-N–H···Cl, one ammonium-N–H···O(carbonyl) and one amino-N–H···Cl hydrogen-bonding interactions.

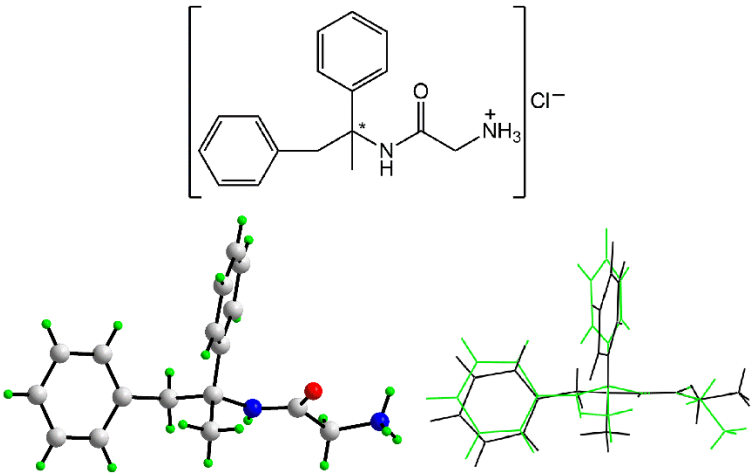

Figure 26.19. Images for [(1,2-diphenylpropan-2-yl)carbamoyl]methanaminium chloride [MAPXUX; **19**]: chemical diagram, molecular structure of the cation and overlay diagram of the independent cations.

A 1:1 ratio between cations and anions is also found in the crystal of 2-((2,8-bis(trifluoromethyl)quinolin-4-yl)(hydroxy)methyl)piperidinium 3,3,3-trifluoro-2-methoxy-2-phenylpropanoate (triclinic, *P*1 with *Z*′ = 2) [49]. The special feature of this structure is that the anions are chiral, each have a *R*-configuration, precluding the adoption of a centrosymmetric space-group. The molecule illustrated in Figure 26.20 has two chiral centres, with the carbon bearing the

hydroxyl group being *S* and the other being *R*. The overlay diagram between this molecule and its pseudo enantiomer mate indicates differences in the relative orientations of the piperidinium cations. The hydrogen-bonding interactions formed by the cations are quite similar, at least to a first approximation, with each of the hydroxyl groups participating in a charge-assisted O–H···O hydrogen-bond with a carboxylate-oxygen atom. Each ammonium-N–H atom is bifurcated. One hydrogen atom from each ammonium each group forms an intramolecular, charge-assisted N–H···O(hydroxyl) hydrogen-bond and the remaining charge-assisted hydrogen-bonds are of the type N–H···O(carboxylate).

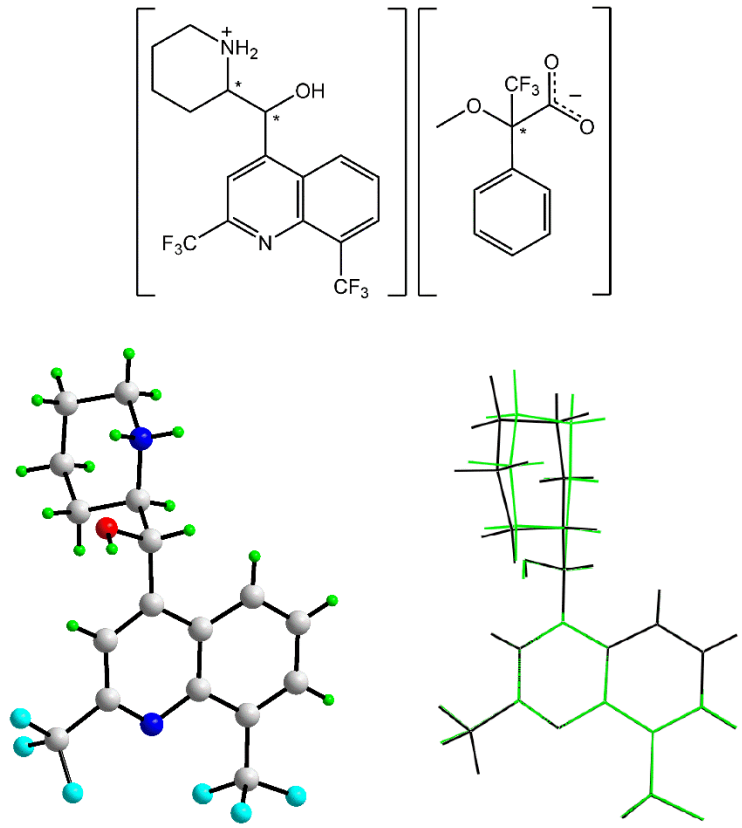

Figure 26.20. Images for 2-{[2,7-bis(trifluoromethyl)quinolin-4-yl](hydroxy)methyl}piperidin-1-ium 3,3,3-trifluoro-2-methoxy-2-phenylpropanoate [ENIPUO; **20**]: chemical diagram, molecular structure of one cation and overlay diagram of the cations.

The next structure to be described is also a 1:1 salt, *i.e.* bis(2-((2,8-bis(trifluoromethyl)quinolin-4-

yl)(hydroxy)methyl)piperidinium) chloride 4-fluorobenzenesulfonate (orthorhombic, $P2_12_12_1$ with $Z' = 2$) [50]. The key difference in this case is that the two anions are distinct. For the molecule illustrated in Figure 26.21, the chirality of the carbon connected to the hydroxyl group is *R* and the other chiral centre in the ring is *S*. As for **20**, there is a minor conformational difference in the piperidinium cations. Despite the presence of distinct anions, the hydrogen-bonding interactions at play in the crystal are comparable. Thus, each hydroxyl groups forms a hydrogen-bond to a sulphoxide-oxygen atom, indeed to the same atom. The two ammonium-N-H atoms of each cation form charge-assisted hydrogen-bonds to a chloride and to a sulphoxide-oxygen atom.

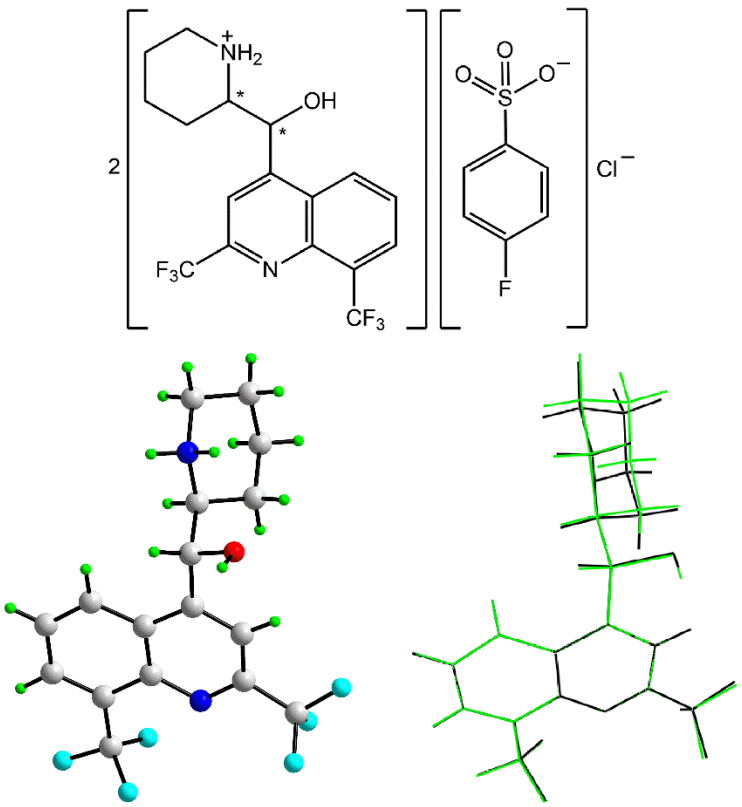

Figure 26.21. Images for 2-{[2,7-bis(trifluoromethyl)quinolin-4-yl](hydroxy)methyl}piperidin-1-ium chloride 4-fluorobenzene-1-sulfonate [ELAMAH, **21**]: chemical diagram, molecular structure of one cation and overlay diagram.

The crystal of **21** is the second 2-{[2,7-bis(trifluoromethyl)quinolin-4-yl](hydroxy)methyl}piperidin-1-ium salt to be described. These species are of interest as the *R*,*S*-cation, as its chloride

salt, commonly known as mefloquinium chloride, was found to be effective against malaria [51]. The salts **20** and **21** were prepared in attempts to resolve the enantiomers as the *S*,*R*-enantiomer causes toxic side-effects and, in fact, were the structures that piqued the interest of the author in this field. Of the about 30 known [4] crystal structures of methloquine/mefloquinium, two are kryptoracemic. In another study [52], where crystallographic details were reported only extremely briefly, it was mentioned that in their attempts at chiral resolution, about the same ratio of kryptoracemates were isolated. These numbers exceed greatly the estimated 0.1% frequency for this behaviour and may suggest a propensity of these molecules towards kryptoracemic behaviour. However, it is more likely that the "McCrone axiom" is apt here [53]: paraphrasing, the more effort one puts into discovering different forms of crystals, the more likely it is that new forms will be discovered. This axiom is clearly vindicated by computational chemistry investigations which indicate that many calculated polymorphic forms of a molecule may differ in Gibbs free energies by only a few kcal/mol [54, 55].

One last kryptoracemate example is included for the sake of completeness, namely a salt solvate, *cis*-2-phenyl-3-methoxycarbonyl-pyrrolidinium oxalate hemihydrate (22) [56]. The crystallographic asymmetric unit in the monoclinic space-group $P2_1$ comprises two cations, two anions and a water molecule of crystallisation. The cation represented in Figure 26.22 has *S*- and *R*-configurations at the carbon atoms carrying the phenyl and ester groups, respectively. As is normally the case, the agreement in conformation between the illustrated and inverted mate is close as seen in the overlay diagram. The hydrogen-bonding profiles exhibited by the cations are quite similar with one ammonium-N–H atom of each forming a donor interaction to the water molecule of crystallisation. In the same way, the second ammonium-N–H atom of each cation is bifurcated. For the illustrated molecule in Figure 26.22, this atom bridges the carbonyl-oxygen atom of the carboxylic acid group and a carboxylate-oxygen atom of the same oxalate anion, thereby forming a five-membered {H···OCCO} synthon. A slight difference occurs in the case of the second cation. Although a five-membered {H···OCCO} synthon is still formed, one, weaker, hydrogen-bond involves the hydroxy group

of the oxalate anion (rather than a carbonyl) resulting in a significantly longer N–H···O hydrogen-bond.

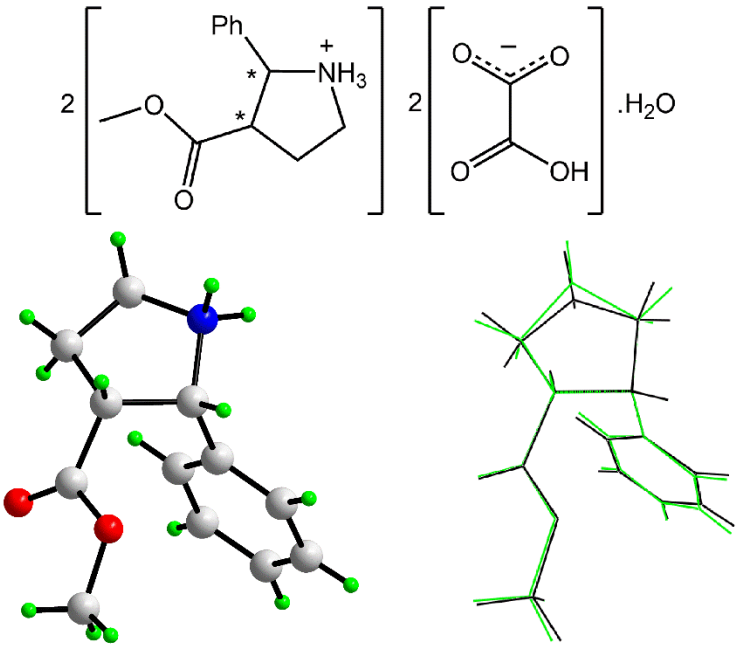

Figure 26.22. Images for 3-(methoxycarbonyl)-2-phenylpyrrolidin-1-ium hydrogen oxalate hemihydrate [FAHQUB; **22**]: chemical diagram, molecular structure of one of the cations and overlay diagram of the cations.

26.4 Overview

The intention of the present survey of reported kryptoracemic crystals highlights the structural diversity of this rare class of crystal,

making up only 0.1% of all-organic crystals [3]. The genuine or pure kryptoracemates – containing pseudo-racemic pairs only – have molecules related about a non-crystallographic centre of symmetry with only minor conformational differences. Similar observations pertain to non-genuine kryptoracemates which contain additional species (solvent and counter-ions) in their crystals in addition to pseudo-racemic pairs. Kryptoracemates can only crystallise in Sohncke space-groups and the overwhelming majority of genuine examples crystallised in three space-groups: $P1$ (15%), $P2_1$ (52%) or $P2_12_12_1$ (33%). For the non-genuine kryptoracemates, a possible reason for this behaviour may relate to the presence of additional species and the influence these have on the supramolecular association operating in the crystals, something unlikely to "pertain" in the genuine kryptoracemates.

At present, it is probably fair to opine that most of the reported kryptoracemates are the product of serendipity and that systematic studies are likely to uphold the McCrone axiom [53] but, prove to be most rewarding at the same time [57]. Certainly, a rationale of this

behaviour will prove useful in the understanding of the crystallisation phenomenon in general.

References

1. G.A. Morales, F.R. Fronczek, A kryptoracemic hydroperoxide. Acta Crystallogr. **C52**, 1266–1268 (1996).
2. I. Bernal, ACA Annual Meeting, Montreal, Quebec, Canada. Abstract 4a.1.e (1995).
3. L. Fábián, and C.P. Brock, A list of organic kryptoracemates. Acta Crystallogr. **B66**, 94–103 (2010).
4. R. Taylor, P.A. Wood, A million crystal structures: The whole is greater than the sum of its parts. Chem. Rev. **119**, 9427–9477 (2019).
5. I. Bernal and S. Watkins, A list of organometallic kryptoracemates. Acta Crystallogr. **C71**, 216–221 (2015).
6. B. Dalhus, C.H. Görbitz, Non-centrosymmetric racemates: space-group frequencies and conformational similarities between crystallographically independent molecules. Acta Crystallogr. **B56**, 715–719 (2000).

7. H.D. Flack, Louis Pasteur's discovery of molecular chirality and spontaneous resolution in 1848, together with a complete review of his crystallographic and chemical work. Acta Crystallogr. **A65**, 371–389 (2009).

8. L. Pérez-García, D.B. Amabilino, Spontaneous resolution, whence and whither: from enantiomorphic solids to chiral liquid crystals, monolayers and macro- and supra-molecular polymers and assemblies. Chem. Soc. Rev. **36**, 941–967 (2007).

9. E. Pidcock, W.D.S. Motherwell, J.C. Cole, A database survey of molecular and crystallographic symmetry. Acta Crystallogr. **B59**, 634–640(2003).

10. C.P. Brock, J.D. Dunitz, Towards a grammar of crystal packing. Chem. Mater. **6**, 1118–1127 (1994).

11. H.D. Flack, Chiral and achiral crystal structures. Helv. Chim. Acta **86** 905–921 (2003).

12. B. Moulton, M.J. Zaworotko, From molecules to crystal engineering: Supramolecular isomerism and

polymorphism in network solids. Chem. Rev. **101**, 1629–1658 (2001).

13. J.-P. Zhang, X.-C. Huang, X.-M. Chen, Supramolecular isomerism in coordination polymers. Chem. Soc. Rev. **38**, 2385–2396 (2009).

14. A.J. Cruz-Cabeza, S.M. Reutzel-Edens, J. Bernstein, Facts and fictions about polymorphism. J. Chem. Soc. Rev. **44**, 8619–8635 (2015).

15. S.R. Hall, F.H. Allen, I.D. Brown, The Crystallographic Information File (CIF): A new standard archive file for crystallography. Acta Crystallogr. **A47**, 655–685 (1991).

16. K. Brandenburg, H. Putz, DIAMOND - Crystal and molecular structure visualization. Crystal Impact GbR: Bonn, Germany (2006).

17. J.D. Gans, D. Shalloway, Qmol: A program for molecular visualization on Windows-based PCs. J. Molec. Graphics Model. **19**, 557–559 (2001).

18. C.F. Macrae, P.R. Edgington, P. McCabe, E. Pidcock, G.P. Shields, R. Taylor, M. Towler, J. van de Streek,

Mercury: Visualization and analysis of crystal structures. J. Appl. Cryst. **39**, 453–457 (2006).

19. A.L. Spek, Structure validation in chemical crystallography. Acta Crystallogr. **D65**, 148–155 (2009).
20. ChemAxon (2010). Marvinsketch. http://www.chemaxon.com (accessed November 1st, 2019)
21. A. Mostad, C. Romming, L. Tressum, The crystal and molecular structure of (2-hydroxyphenyl)alanine (o-tyrosine). Acta Chem. Scand. **29**, 171–176 (1975).
22. T. Patonay, J. Jekó, E. Juhász-Tóth, Synthesis of highly substituted 2H-azirine-2-carboxylates via 3-Azido-4-oxo-but-2-enoates. Eur. J. Org. Chem. **125**, 1441–1448 (2008).
23. V.M. Berestovitskaya, I.A. Litvinov, I.E. Efremova, L.V. Lapshina, D.B. Krivolapov, A.T. Gubaidullin, Halo derivatives of 2,4-dinitrothiolene 1,1-dioxides: Synthesis and structure. Russ. J. Gen. Chem. **72**, 1111–1118 (2002).
24. A. Ohsawa, H. Arai, H. Ohnishi, T. Kaihoh, T. Itoh, K. Yamaguchi, H. Igeta, Y. Iitaka, Sodium borohydride

reduction of 1,2,3-triazine derivatives. J. Pharm. Soc. Jpn. **105**, 1122–1130 (1985).

25. S. Erhardt, S.A. Macgregor, K.J. McCullough, K. Savill, B.J. Taylor, Model studies of β-scission ring-opening reactions of cyclohexyloxy radicals: Application to thermal rearrangements of dispiro-1,2,4-trioxanes. Org. Lett. 5569–5572 (2007).

26. K.J. McCullough, M.B. Hursthouse, S.J. Coles, Private communication to the Cambridge Structural Database. Refcode NIWHUX01 (1993).

27. B.D. Santarsieroa, Richard E. Marsh (1922–2017). Acta Crystallogr. **C73**, 1038-1039 (2017).

28. R.E. Marsh, The importance of weak reflections in resolving the centrosymmetric-noncentrosymmetric ambiguity: a cautionary tale. Acta Crystallogr. **B37**, 1985–1988 (1981).

29. R.E. Marsh, A.L. Spek, Use of software to search for higher symmetry: space group C2. *Acta Crystallogr.* **B57**, 800–805 (2001).

30. Steed, K.S., Steed, J.W., Packing problems: High Z' crystal structures and their relationship to cocrystals, inclusion compounds, and polymorphism. Chem. Rev. **115**, 2895–2933 (2015).

31. M.K.J. ter Wiel, R.A. van Delden, A. Meetsma, B.L. Feringa, Increased speed of rotation for the smallest light-driven molecular motor. J. Am. Chem. Soc. **125**, 15076–15086 (2003).

32. D.J. Aitken, C. Gauzy, E. Pereira, A short synthesis of the cis-cyclobutane β-aminoacid skeleton using a [2+2] cycloaddition strategy. Tetrahedron Lett. **43**, 6177–6179 (2002).

33. F.H. Allen, W.D.S. Motherwell, P.R. Raithby, G.P. Shields, R. Taylor, Systematic analysis of the probabilities of formation of bimolecular hydrogen-bonded ring motifs in organic crystal structures. New J. Chem. **23**, 25–34 (1999).

34. E.R.T. Tiekink, Supramolecular assembly based on “emerging” intermolecular interactions of particular

interest to coordination chemists. Coord. Chem. Rev. **345**, 209–248 (2017).

35. S. Beşli, S.J. Coles, D.B. Davies, M.B. Hursthouse, H. Ibişoğlu, A. Kiliç, R.A. Shaw, Retention of configuration in the nucleophilic substitution reactions of some nine-membered ansa derivatives of cyclotriphosphazatriene. Chem. Eur. J. **10**, 4915–4920 (2004).

36. A. Furusaki, K. Abe, T. Matsumoto, X-Ray Structure of (1RS, 5RS, 7SR)-1-acetoxy-7-cyano-5-methylbicyclo[3.2.0]heptan-2-one, a photocycloadduct of 2-acetoxy-3-methyl-2-cyclopenten-1-one and acrylonitrile. Bull. Chem. Soc. Jpn. **55**, 611–612 (1982).

37. I. Coldham, A.J.M. Burrell, L.E. White, H. Adams, N. Oram, Highly efficient synthesis of tricyclic amines by a cyclization/cycloaddition cascade: total syntheses of aspidospermine, aspidospermidine, and quebrachamine. Angew. Chem., Int. Ed. **46**, 6159–6162 (2007).

38. R. Savinsky, H. Hopf, I. Dix, P.G. Jones, Partially hydrogenated [2.2]paracyclophanes as precursors in polycyclic

hydrocarbon chemistry. Eur. J. Org. Chem. 4595–4606 (2001).

39. K.-J. Su, J.-L. Mieusset, V.B. Arion, L. Brecker, U.H. Brinker, Cope rearrangement versus a novel tandem retro-Diels−Alder−Diels−Alder reaction with role reversal. Org. Lett. **9**, 113–115 (2007).

40. M. Kalesse, R. Wartchow, Structural features for the promotion of optimal stacking in the solid state. Tetrahedron **54**, 8015–8024 (1998).

41. Z. Gültekin, T. Hökelek, Crystal Structure of *trans*-(1*RS*,3*RS*)-2-*N*,*N*′-Dimethylaminomethyl-1,3-dithiolane-1,3-dioxide. Anal. Sci.: X-Ray Struct. Anal. Online **22**, x9–x10 (2006).

42. M.J. Heileman, H.W. Moore, Generation and intramolecular cyclization of (2-ethenylphenyl)bisketenes. Synthesis of benzofuranones. Tetrahedron Lett. **39**, 3643–3646 (1998).

43. A. Basak, S.S. Bag, P.A. Mazumdar, V. Bertolasi, A.K. Das, Molecular recognition in β-lactams: The crystal

packing in 4-sulfonyl β-lactams. J. Chem. Res. 318–321 (2004).

44. V. Sharma, J.J. Tepe, Diastereochemical diversity of imidazoline scaffolds via substrate controlled TMSCl mediated cycloaddition of azlactones. Org. Lett. **7**, 5091–5094 (2005).

45. C.P. Brock, L.L. Duncan, Anomalous space-group frequencies for monoalcohols, C_nH_mO. Chem. Mater. **6**, 1307–1312 (1994).

46. J.A. Bis, P. Vishweshwar, D. Weyna, M.J. Zaworotko, Hierarchy of supramolecular synthons: Persistent hydroxyl···pyridine hydrogen bonds in cocrystals that contain a cyano acceptor. Molec. Pharma. **4**, 401–416 (2007).

47. A.M. Al-Khashashneh, M.M. El-Abadelah, R. Boese, Novel synthesis of model dihydroazepine-fused indolo[2,3-c]quinolines. Heterocycles **60**, 73–87 (2003).

48. G.R. Lewis, G. Steele, L. McBride, A.J. Florence, A.R. Kennedy, N. Shankland, W.I.F. David, K. Shankland, S.J. Teat, Hydrophobic vs. hydrophilic: Ionic competition in

remacemide salt structures. Cryst. Growth Des. **5**, 427–438 (2005).

49. J.L. Wardell, S.M.S.V. Wardell, E.R.T. Tiekink, A kryptoracemic salt: 2-{[2,8-bis(trifluoromethyl)quinolin-4-yl](hydroxy)methyl}piperidin-1-ium (+)-3,3,3-trifluoro-2-methoxy-2-phenylpropanoate. *Acta Crystallogr.* **E57**, 872–877 (2016).

50. M.M. Jotani, J.L. Wardell, E.R.T. Tiekink, Crystal structure and Hirshfeld analysis of the kryptoracemate: bis(mefloquinium) chloride p-fluorobenzenesulphonate. Z. Kristallogr. Cryst. Mater. **231**, 247–255 (2016).

51. R.L. Nevin, A serious nightmare: psychiatric and neurologic adverse reactions to mefloquine are serious adverse reactions. Pharmacol. Res. Perspect. **5**, e00328 (2017).

52. A.H.J. Engwerda, R. Maassen, P. Tinnemans, H. Meekes, F.P.J.T. Rutjes, E. Vlieg, Attrition-enhanced deracemization of the antimalaria drug mefloquine.Angew. Chem. Int. Ed. **58**, 1670–1673 (2019).

53. J. Haleblian, W. McCrone, Pharmaceutical applications of polymorphism. J. Pharm. Sci. **58**, 911–929 (1969).

54. A. Gavezzotti, G. Filippini, Polymorphic forms of organic crystals at room conditions: Thermodynamic and structural implications. J. Am. Chem. Soc. **117**, 12299–12305 (1995).

55. S.L. Price, Is zeroth order crystal structure prediction (CSP_0) coming to maturity? What should we aim for in an ideal crystal structure prediction code? *Faraday Discuss*. **211**, 9–30 (2018).

56. S. Suresh, M. Periasamy, Synthesis of *cis*-2-aryl-3-pyrrolidine carboxylic esters via diastereoselective cyclization of γ-imino esters using a $TiCl_4/Et_3N$ reagent system. Tetrahedron Lett. **45**, 6291–6293 (2004).

57. R. Laubenstein, M.-D. Şerb, U. Englert, G. Raabe, T. Braun, B. Braun, Is it all in the hinge? A kryptoracemate and three of its alternative racemic polymorphs of an aminonitrile. Chem. Commun. **52**, 1214–1217 (2016).